Proof-of-principle direct measurement of particle statistical phase

Yan Wang,[1,2,3] Matteo Piccolini,[4,5,*] Ze-Yan Hao,[1,2,3] Zheng-Hao Liu,[1,2,3] Kai Sun,[1,2,3,†] Jin-Shi Xu,[1,2,3,‡] Chuan-Feng Li,[1,2,3,§] Guang-Can Guo,[1,2,3] Roberto Morandotti,[5] Giuseppe Compagno,[6] and Rosario Lo Franco[4,¶]

[1] *CAS Key Laboratory of Quantum Information, University of Science and Technology of China, Hefei 230026, China*
[2] *CAS Center for Excellence in Quantum Information and Quantum Physics, University of Science and Technology of China, Hefei 230026, China*
[3] *Hefei National Laboratory, University of Science and Technology of China, Hefei 230088, China*
[4] *Dipartimento di Ingegneria, Università di Palermo, Viale delle Scienze, 90128 Palermo, Italy*
[5] *INRS-EMT, 1650 Boulevard Lionel-Boulet, Varennes, Québec J3X 1S2, Canada*
[6] *Dipartimento di Fisica e Chimica - Emilio Segrè, Università di Palermo, via Archirafi 36, 90123 Palermo, Italy*

The symmetrization postulate in quantum mechanics is formally reflected in the appearance of an exchange phase ruling the symmetry of identical particle global states under particle swapping. Many indirect measurements of this fundamental phase have been reported thus far, while a direct observation has been only recently achieved for photons. Here we propose a general scheme capable of directly measuring the exchange phase of any type of particles (bosons, fermions, anyons), exploiting the operational framework of spatially localized operations and classical communication. We experimentally implement it in an all-optical platform providing proof-of-principle for different simulated exchange phases. As a byproduct, we supply a direct measurement of the real bosonic exchange phase of photons. Additionally, we analyze the performance of the proposed scheme when mixtures of particles of different natures are injected. Our results confirm the symmetrization tenet and provide a tool to explore it in various scenarios. Finally, we show that the proposed setup is suited to generate indistinguishability-driven N00N states useful for quantum-enhanced phase estimation.

The symmetrization postulate divides particles living in a 3-dimensional space into two groups: bosons and fermions. Such a postulate forces the state of an ensemble of identical bosons (fermions) to be symmetric (antisymmetric) under the exchange of any pair of particles [1]. Considering a system of two identical particles, its global state must then satisfy $|\psi(1,2)\rangle = e^{i\phi}|\psi(2,1)\rangle$, where 1 and 2 refer to the two constituents and the relative phase ϕ is the particle exchange phase (EP), with $\phi = 0$ for bosons and $\phi = \pi$ for fermions. Furthermore, the existence of particles called anyons living in 2-dimensional spaces with a fractional EP $\phi \in (0, 2\pi) \setminus (\pi)$ has been suggested [2, 3], attracting the attention of the scientific community in recent decades [4–6]. This fundamental phase has been indirectly measured by various experiments [7–12]. Despite the fundamental importance of the symmetrization postulate in both understanding the quantum world and practical applications, only the bosonic nature of photons has been so far directly proven by a state transport protocol [13, 14]. A direct observation of fermionic and anyonic EPs is still missing, leaving the field open to the introduction of new techniques capable to fill that gap.

In the standard approach to identical particles [1] the global state vector is symmetrized or antisymmetrized with respect to unphysical labels associated to each constituent. This approach is known to exhibit drawbacks when trying to assess real quantum correlations between constituents [15, 16]. Given the key role played by entanglement in quantum technologies, different methods have been developed to fix such an issue [16–23]. Among these, the no-label approach [21] provides some advantages: it straightforwardly identifies physical entanglement and establishes its quantitative relation with the degree of spatial indistinguishability [24]; the latter is associated to the spatial overlap of particle wave functions. Importantly, in the no-label formalism, the role played by the particles' nature does not manifest itself in the (anti)symmetrization of the quantum state but in the probability amplitudes of the global system [21, 22].

The no-label approach has been widely exploited within spatially localized operations and classical communication (sLOCC) environments [23–31]. Such a procedure can be seen as a natural extension of standard local operations and classical communication (LOCC) for distinguishable particles to the case of indistinguishable and individually unaddressable constituents. Operationally, sLOCC makes the global state of indistinguishable particles undergo a projective measurement over spatially-separated regions, followed by a post-selection when one particle is found in each location. Consider a state of two independent identical qubits $|\psi_{\rm D}\rangle = |\varphi_{\rm D}\uparrow, \varphi'_{\rm D}\downarrow\rangle$, where $\varphi_{\rm D}$, $\varphi'_{\rm D}$ are spatial wave functions and $\uparrow, \downarrow$ are pseudospins. The result of sLOCC onto $|\psi_{\rm D}\rangle$ gives [23]

$$|\psi_{\rm LR}\rangle = \frac{lr'\,|{\rm L}\uparrow, {\rm R}\downarrow\rangle + e^{i\phi} rl'\,|{\rm L}\downarrow, {\rm R}\uparrow\rangle}{\sqrt{|lr'|^2 + |rl'|^2}}, \qquad (1)$$

where l, l' (r, r') are the probability amplitudes for each particle to be found in the region L (R), while ϕ is the exchange (statistical) phase; $|\psi_{\rm LR}\rangle$ is entangled only if the qubits spatially overlap, i.e., are spatially indistinguish-

able, at the regions L and R. Remarkably, the sLOCC process makes particle statistics naturally emerge in the final entangled state. The entanglement obtained is experimentally accessible [29, 30], and has been exploited for teleportation [29] and phase discrimination [31]. Also, sLOCC-based indistinguishability is useful for protecting entanglement against noise [24, 26–28].

Here we give further value to sLOCC by experimentally showing, in a quantum-optical setup, that its theoretical framework enables a phase-estimation procedure to directly access the EPs of indistinguishable particles of any nature (Fig. 1(a)).

Theoretical background. The conceptual procedure is depicted in Fig. 1(a). Let us take a pair of two-level identical particles independently prepared and initially uncorrelated, whose spatial wave functions and pseudospins are respectively $\varphi, \uparrow$ and $\varphi', \downarrow$. In the no-label formalism, we write this state as $|\psi_{\rm in}\rangle = |\varphi\uparrow, \varphi'\downarrow\rangle$. Then, a deformation operation $|\varphi\rangle \to |\varphi_{\rm D}\rangle$, $|\varphi'\rangle \to |\varphi'_{\rm D}\rangle$ is performed [24, 26, 32] to distribute the spatial wave functions over two distinct regions L and R in a controllable way, thus transforming $|\psi_{\rm in}\rangle$ into $|\psi_{\rm D}\rangle = |\varphi_{\rm D}\uparrow, \varphi'_{\rm D}\downarrow\rangle$, where

$$|\varphi_{\rm D}\rangle = l\,|{\rm L}\rangle + r\,|{\rm R}\rangle\,, \quad |\varphi'_{\rm D}\rangle = l'\,|{\rm L}\rangle + r'\,|{\rm R}\rangle\,. \tag{2}$$

Here, the coefficients $l = \langle {\rm L}|\varphi_{\rm D}\rangle$, $l' = \langle {\rm L}|\varphi'_{\rm D}\rangle$, $r = \langle {\rm R}|\varphi_{\rm D}\rangle$ and $r' = \langle {\rm R}|\varphi'_{\rm D}\rangle$ are the tunable probability amplitudes of finding the particle whose spatial wave function is φ_D or φ'_D in the site L and R, respectively.

To implement the sLOCC measurement we perform the post-selected detection of the states where exactly one qubit per region is recorded. In total, this last step amounts to projecting the state $|\psi_D\rangle$ onto the two particle basis $\mathcal{B}_{\rm LR} = \{|{\rm L}\uparrow,{\rm R}\uparrow\rangle, |{\rm L}\uparrow,{\rm R}\downarrow\rangle, |{\rm L}\downarrow,{\rm R}\uparrow\rangle, |{\rm L}\downarrow,{\rm R}\downarrow\rangle\}$ via the projection operator $\hat{\Pi}_{\rm LR} = \sum_{\sigma,\tau=\uparrow,\downarrow} |{\rm L}\sigma,{\rm R}\tau\rangle\langle {\rm L}\sigma,{\rm R}\tau|$.

We recall that the two particles in the state $|\psi_D\rangle$ are indistinguishable to the eyes of the detectors. This means that it is not possible to know the region of space where each detected constituent comes. Such no which-way information is encoded in the result of the sLOCC operation, which is easily computed to be the (normalized) two-particle entangled state

$$\begin{aligned} |\psi_{\rm LR}\rangle &= \frac{\hat{\Pi}_{\rm LR}\,|\psi_D\rangle}{\sqrt{\langle\psi_D|\,\hat{\Pi}_{\rm LR}\,|\psi_D\rangle}} \\ &= \frac{lr'\,|{\rm L}\uparrow,{\rm R}\downarrow\rangle + e^{i\phi} rl'\,|{\rm L}\downarrow,{\rm R}\uparrow\rangle}{\sqrt{|lr'|^2+|rl'|^2}}, \end{aligned} \tag{3}$$

generated with probability $P_{\rm LR} = |lr'|^2 + |rl'|^2$ [23]. The naturally emerged phase ϕ in Eq. (3) is exactly the relative EP we want to measure (Fig. 1(a)). In fact, it is fundamentally contained in the probability amplitudes $\langle\chi_{\rm L},\chi_{\rm R}|\,\psi_{\rm D}\rangle = \langle\chi_{\rm L}|\,\chi_{\rm D}\rangle\langle\chi_{\rm R}|\,\chi'_{\rm D}\rangle + \eta\,\langle\chi_{\rm L}|\,\chi'_{\rm D}\rangle\langle\chi_{\rm R}|\,\chi_{\rm D}\rangle$ [21], where $\chi_{\rm L} = {\rm L}\sigma$, $\chi_{\rm R} = {\rm R}\tau$, $\chi_{\rm D} = \varphi_{\rm D}\uparrow$, $\chi'_{\rm D} = \varphi'_{\rm D}\downarrow$ and $\eta = e^{i\phi}$ is the particle statistics parameter. It is worth highlighting that the state $|\psi_{\rm LR}\rangle$, resulting from the sLOCC process, describes two particles occupying two distinct regions of space, thus being now distinguishable and individually addressable. The spatial indistinguishability $\mathcal{I}$ under sLOCC associated to the state $|\psi_{\rm D}\rangle$, and thus to the state $|\psi_{\rm LR}\rangle$, is given by [24]

$$\begin{aligned} \mathcal{I} = &-\frac{|lr'|^2}{|lr'|^2+|l'r|^2}\log_2\frac{|lr'|^2}{|lr'|^2+|l'r|^2} \\ &-\frac{|l'r|^2}{|lr'|^2+|l'r|^2}\log_2\frac{|l'r|^2}{|lr'|^2+|l'r|^2}. \end{aligned} \tag{4}$$

In general, the state of Eq. (3) represents a quantum superposition of two-particle states whose relative phase contains the EP of the particles. Notice that one of the major difficulties in directly measuring the particle statistical phase consists in creating quantum interference between a given state and its counterpart where particles have been physically exchanged [14]. A so-called state-dependent transport protocol has been first engineered to this aim [33] and successively realized with photons [13]. On the other hand, in our scheme, the fundamental EP straightforwardly appears as a natural consequence of spatial overlap at separated regions plus the sLOCC procedure, making it amenable to be directly measured via individual operations on the particles. We then proceed by rotating the pseudospin of both qubits by $\pi/4$. Given the single particle operator

$$\hat{M}_X = \frac{1}{\sqrt{2}}\begin{pmatrix} 1 & -1 \\ 1 & 1 \end{pmatrix}, \tag{5}$$

performing such operation on the region $X = L, R$, the resulting state is given by $|\psi_f\rangle = \hat{M}_{\rm L}\otimes\hat{M}_{\rm R}\,|\psi_{\rm LR}\rangle$. Finally, a direct measurement of the pseudospin along the z-axis in both regions L and R provides information about the EP. Indeed, we find that

$$\langle\psi_f\,|\hat{\sigma}^z_{\rm L}\otimes\hat{\sigma}^z_{\rm R}|\,\psi_f\rangle = \frac{2lr'rl'}{|lr'|^2+|rl'|^2}\cos\phi, \tag{6}$$

where we have taken the coefficients l, r, l', r' to be real since we are able to directly control the distribution of the initial spatial wave functions over L and R during the preparation of the state $|\psi_{\rm D}\rangle$. By knowing such amplitudes, it is thus possible to recover the value of the EP from repeated pseudospin measurements along the z-axis.

Remarkably, the role of spatial indistinguishability $\mathcal{I}$ clearly emerges from Eq. (6): indeed, as its value varies from $\mathcal{I} = 1$ (maximum indistinguishability, obtained, e.g., when $l = r = l' = r' = 1/\sqrt{2}$) to $\mathcal{I} = 0$ (distinguishable particles, e.g., when $l = r' = 1$, $l' = r = 0$) [24], the values assumed by Eq. (6) continuously change from $\cos\phi$ to zero, correspondingly. It follows that spatial indistinguishability is not only an essential element

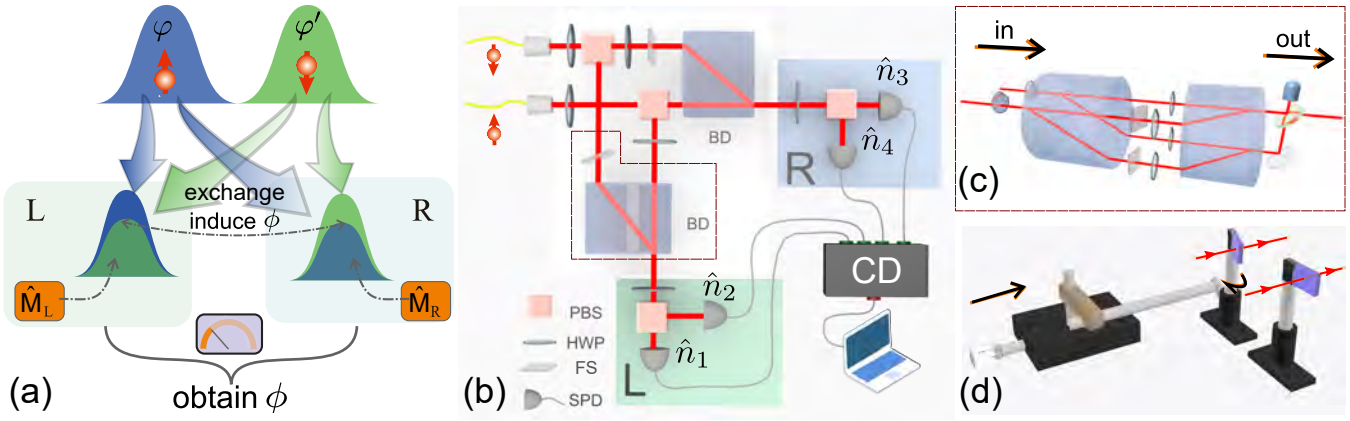

FIG. 1. Theoretical scheme and experimental setup. (a) Conceptual procedure. The wave functions of two identical particles are distributed over two distinct regions L and R and adjusted to spatially overlap, generating spatial indistinguishability. A sLOCC measurement is used to directly observe the EP using a single-particle rotation $\hat{M}$ in the two regions. (b) Experimental setup. Two independently prepared photons with opposite polarizations are distributed to two distinct spatial regions L and R, respectively. In each region, a beam displacer (BD) is used to merge two beams, generating spatial indistinguishability between the two photons. The relative phase between two spatial modes of photons is properly tuned using a phase adjustment consisting of the fused silicon (FS) shown in (d). The four outputs are individually directed towards four single-photon detectors (SPDs), where a coincidence device (CD) is used to deal with the signals. PBS: polarization beam splitter, HWP: half-wave plate. (c) Replacement setup for the dashed frame in (b). The unbalanced interferometer is used to prepare the mixed states.

for measuring the EP with our procedure, but it also acts as a sensibility regulator which tunes our ability to access the value of ϕ.

Experiment. Denoting with $|H\rangle$ and $|V\rangle$ the horizontal and vertical polarization of a photon, respectively, we make the correspondence $|H\rangle \leftrightarrow |\uparrow\rangle$ and $|V\rangle \leftrightarrow |\downarrow\rangle$. A pulsed ultraviolet beam with wavelength at 400 nm is used to pump a type-II phase-matched β-barium borate (BBO) crystal to generate two uncorrelated photons ($|H\rangle\otimes|V\rangle$) via spontaneous parametric down conversion. Hong-Ou-Mandel interference is performed to characterize the indistinguishability of the two photons, providing a visibility of 97.7% [29]. Single-mode fibers collect the photons via fiber couplers and direct them towards the effective experimental setup illustrated in Fig. 1(b). Here, the weights of their horizontal and vertical polarizations are tuned using a pair of half wave plates (HWPs) fixed at 22.5° and $-\beta/2$ (adjustable angle), respectively. An additional pair of HWPs at 45° is placed on L to restore the original input polarizations. The result is the preparation of the state $|\psi_{\rm D}\rangle$ with $|\varphi_D\rangle = (|{\rm L}\rangle + |{\rm R}\rangle)/\sqrt{2}$, $|\varphi'_D\rangle = \sin\beta\,|{\rm L}\rangle + \cos\beta\,|{\rm R}\rangle$.

Using a home-made phase adjustment composed of a thin plate of fused silicon (FS) fixed in R and of another identical plate tilted and placed in L (Fig.1(b), (d)), an arbitrary relative phase ϕ_s is judiciously introduced between the components L and R of the photon φ'_D, which becomes $|\varphi'_D\rangle = e^{i\phi_s}\sin\beta\,|{\rm L}\rangle + \cos\beta\,|{\rm R}\rangle$. As shown in Fig. 1(d), ϕ_s is tuned by directly adjusting the distance x (mm) of a movable plate. The relation between ϕ_s and x is displayed in Fig. 2(a) with experimental results (dots) and theoretical prediction (solid line) with a plate's thickness $d = 199.94 \pm 1.43$ μm and a rotation radius $r = 102.36 \pm 0.91$ mm (Supplementary note I).

A beam displacer (BD) is used to make the two beams overlap over both regions. We proceed by setting an HWP at 22.5° after the BD in both L and R to implement the desired rotation, producing the final state $|\psi_f\rangle$. The pseudospin measurement $\hat{\sigma}_z^{(L)} \otimes \hat{\sigma}_z^{(R)}$ is then performed as a coincidence counting by placing each polarization beam splitter (PBS) on both regions L and R. And each output of PBS is individually directed towards a single-photon detector. The corresponding measured observable is

$$\langle \hat{O} \rangle = \hat{n}_{13} + \hat{n}_{24} - \hat{n}_{14} - \hat{n}_{23}, \tag{7}$$

where $\hat{n}_{ij}$ is the coincidence count between the outputs $\hat{n}_i$ and $\hat{n}_j$ which are shown in Fig. 1(b). This spatially localized operation (sLO), implemented through local counting on L and R, and classical communication (CC) tools, realized via the coincidence device, create the state of Eq. (1) with $l = r = 1/\sqrt{2}$, $l' = \sin\beta$, $r' = \cos\beta$, i.e.,

$$|\psi_{\rm LR}\rangle = \cos\beta\,|{\rm L}H, {\rm R}V\rangle + e^{i\phi_s}\sin\beta\,|{\rm L}V, {\rm R}H\rangle\,, \tag{8}$$

before the final rotation transforms it into $|\psi_f\rangle$. Notice that the relative phase ϕ_s in Eq. (8) plays the exact same role of the real EP ϕ in Eq. (3) (which here is set to zero since our experiment is run by bosons). Changing ϕ_s amounts to simulating the behaviour of identical particles with different natures. In other words, the validity of our setup capable of directly measuring ϕ_s provides a tough advocacy to directly detect the EP of any type of particles. Renaming ϕ the simulated exchange phase, we

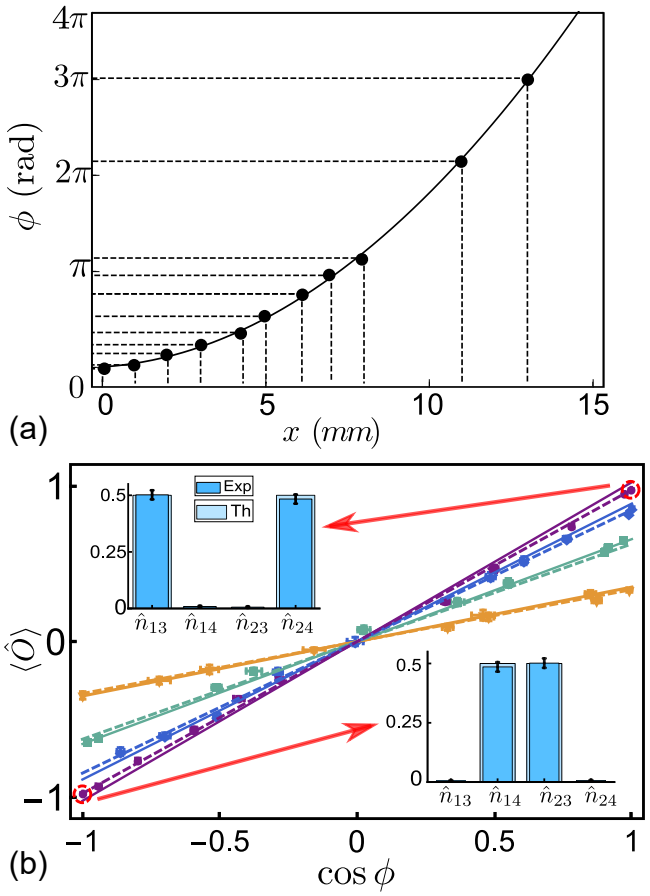

FIG. 2. (a) Relation between the distance x of the moving plate and the generated relative phase ϕ. The black dots represent the experimental results, while the black curve is the theoretical prediction. Errorbars are too small to be visible. (b) Relation between $\langle\hat{O}\rangle$ and $\cos\phi$. Results are reported for different values of β in which the purple, blue, green, and brown colors represent $\beta = 45°$, $30°$, $20°$, and $10°$, respectively. The solid lines represent the ideal expected results, while the dashed lines show the predictions when noise is taken into consideration. Experimental values are represented with markers. The inset two panels show the coincidence counting $\hat{n}_{13}$, $\hat{n}_{14}$, $\hat{n}_{23}$, and $\hat{n}_{24}$ for bosons and fermions, respectively.

obtain

$$\langle\hat{O}\rangle \equiv \langle\psi_f|\,\hat{O}\,|\psi_f\rangle = \sin(2\beta)\cos\phi, \tag{9}$$

from which ϕ can be easily achieved.

We set $\beta = 45°$ and $\phi = 0$ to prepare two maximally indistinguishable photons (bosons), generating maximum entanglement $|\psi_{\rm LR}\rangle = (|{\rm L}H,{\rm R}V\rangle + |{\rm L}V,{\rm R}H\rangle)/\sqrt{2}$ with a fidelity of 0.99 ± 0.01. Unavoidable experimental errors prevent the achievement of ideal maximum indistinguishability, which leads to a non-optimal performance of the real setup. Following the method used in Ref. [13], we treat such errors as a constant factor affecting the final experimental results. We assume that the experimentally prepared state is the desired (ideal) one with probability F, while errors give rise to a spoiled state with probability $1-F$. Within this model, the spoiled state does not contribute to the expectation value of $\hat{O}$, leading to the experimentally measured expectation value $\langle\hat{O}\rangle_e = F\langle\hat{O}\rangle_i$ where $\langle\hat{O}\rangle_i$ is the ideal prediction. By preparing several states of Eq. (8) for different values of ϕ, we use quantum state tomography [34] to estimate the probability to be $F = 0.977$ (Supplementary note II).

The two inset panels in Fig. 2(b) show the coincidence counts $\hat{n}_{13}$, $\hat{n}_{14}$, $\hat{n}_{23}$ and $\hat{n}_{24}$ for the cases of (real) bosons and (simulated) fermions, respectively, with $\beta = 45°$. Treating experimental errors following the above introduction, we obtain $\phi_b = 0.04 \pm 0.06$ for bosons and $\phi_f = 3.12 \pm 0.05$ for fermions, which match well with their expected EPs. Here, the errorbar is the standard deviation which is estimated based on the experimental data via the Monte Carlo method.

As shown in Fig. 2(b), by rotating the angle β, we implement various spatial overlaps to provide deeper insights on the role played by spatial indistinguishability in our scheme, and adjust the EPs (including anyonic ones) with the homemade device. The detected values of $\langle\hat{O}\rangle$ are given as a function of $\cos\phi$, in which ϕ is obtained via tomographic measurements, for different degrees of spatial overlap and, hence, of spatial indistinguishability $\mathcal{I} = -\sin^2\beta\log_2(\sin^2\beta) - \cos^2\beta\log_2(\cos^2\beta)$ [24]. The experimental results match quite well with the theoretical predictions. In particular, the case of $\beta = 45°$ corresponds to the maximum spatial overlap ($\mathcal{I} = 1$), while $\beta = 30°$, $\beta = 20°$, $\beta = 10°$ are associated to partial spatial overlaps ($\mathcal{I} < 1$). Notice that when $\mathcal{I}$ decreases, the ranges of values of $\langle\hat{O}\rangle$ decrease accordingly, leading to a lower sensibility. Spatial indistinguishability acts as a sensitive regulator ruling the range of measured values.

As an extension of our framework, we analyze the scenario where the input is a flux of particle pairs whose exchange phase is known to be either ϕ_1 with probability p or ϕ_2 with probability $1-p$. Each two-particle state is thus given by the classical mixture

$$\rho = p\,|\psi_1\rangle\langle\psi_1| + (1-p)\,|\psi_2\rangle\langle\psi_2|\,, \tag{10}$$

where $|\psi_1\rangle = \cos\beta\,|{\rm L}H,{\rm R}V\rangle + e^{i\phi_1}\sin\beta\,|{\rm L}V,{\rm R}H\rangle$ and $|\psi_2\rangle = \cos\beta\,|{\rm L}H,{\rm R}V\rangle + e^{i\phi_2}\sin\beta\,|{\rm L}V,{\rm R}H\rangle$. We now want to exploit our procedure to estimate the probability distribution p of the two types of particles by directly measuring their EPs.

To prepare ρ, we replace the dotted box in Fig. 1(b) with the unbalanced interferometer shown in Fig. 1(c). Here, a BD equipped with two HWPs separately placed on each beam is used to split each beam into two vertical beams. The two upper arms are used to prepare the particle with EP ϕ_1, while two lower arms are used to prepare the particle with EP ϕ_2. By changing the angles of the two HWPs before the BD, the probability distributions p could be adjusted. And as mentioned above,

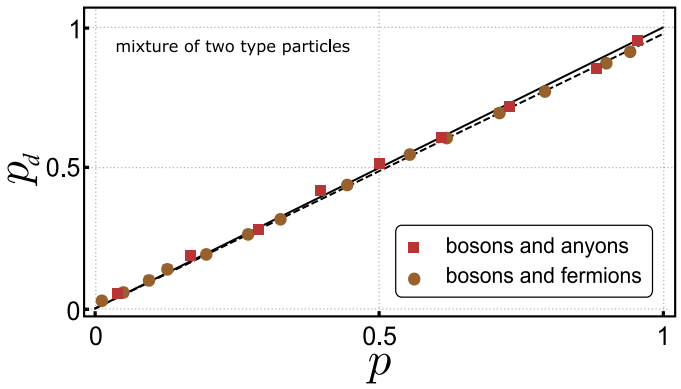

FIG. 3. Probability distribution p_d for a mixture of two-type particles measured by our procedure versus the value p directly generated by rotating HWPs. Experimental results for a mixture of bosons and anyons with EP $\phi = \pi/2$ (red markers), and for a mixture of bosons and fermions (brown markers). Solid lines represent ideal expected values, while dashed lines are the theoretical predictions when noise is considered. Errorbars are too small to be visible.

the EPs ϕ_1 and ϕ_2 are regulated with the corresponding homemade phase adjustment devices. Then, another BD together with several HWPs combines two upper (lower) arms into one beam horizontally. At last, two beams are combined with a beam splitter in which the desired classical mixed state of Eq. (10) is generated in one output and the other output is blocked.

The expectation value $\langle \hat{O} \rangle = \mathrm{Tr}[\rho\, \hat{O}] = p\, \langle \psi_1 |\, \hat{O}\, | \psi_1 \rangle + (1-p)\, \langle \psi_2 |\, \hat{O}\, | \psi_2 \rangle$ is measured following the same method introduced above. For simplicity, we assume that the values of ϕ_1 and ϕ_2 are provided as the prior information, leading to a reduction in $\langle \hat{O} \rangle$ as a linear function of p. Notice that, if this is not the case, the values of ϕ_1 and ϕ_2 can nonetheless be obtained by our procedure to directly measure them on a sufficiently big sample of particles. We start with $\phi_1 = 0$ and $\phi_2 = \pi/2$ to investigate a classical mixture of bosons and anyons with $\beta = 45°$. We generate different probability distributions p by rotating the two HWPs before the first BD as shown in Fig. 1(c). Also, we set $\phi_2 = \pi$ to investigate a mixture of bosons and fermions. The results are reported in Fig. 3, where the detected probability distributions p_d, obtained based on the measured values of $\langle \hat{O} \rangle$, are shown versus the values p directly generated by rotating the HWPs. Excellent agreement with theoretical predictions is observed (Supplementary note III). This latest experiment demonstrates how our procedure can be used to obtain information on the probability distribution p for a mixture of two known different types of particles. If the number of types of particles is increased or unknown, a complete characterization of the incoming flux can still be given by directly measuring the various EPs of the particle pairs composing a sufficiently large sample.

Discussion. In summary, we have experimentally shown that the sLOCC framework is inherently amenable for direct measurement of the EP of indistinguishable particles. Particle statistics in the measured state is entirely due to the spatial indistinguishability achieved via the deformation of particle wave packets. The sLOCC process functions as a trigger making the EP directly accessible within the generated entanglement. For this reason, physical exchange of particles and related geometric phase do not occur here, in contrast with the technique previously adopted [13] to measure the bosonic EP of photons. Our procedure works for bosons, fermions and anyons. We have judiciously designed the optical setup to simulate various particle statistics: different from other methods used for this aim in photonic quantum walks [35, 36], we have manually injected different EPs by accurately tuning a phase adjustment, always observing agreement between measured values and predictions. Our apparatus has confirmed the real bosonic (symmetric) nature of photons, enclosing the result of Ref. [13]. We have also proven that repeated measurements of the EP permit to reconstruct the probability distribution for statistical mixtures of states of particles of different natures. Our work provides a general scheme to directly explore the symmetrization principle and the role of particle statistics in various contexts, which would have extendable applications in other phase measurement schemes [37–39].

As an outlook, it would be interesting to apply our setup in non-optical platforms to achieve the first direct measurement of real (not simulated) fermionic and anyonic EPs. In fact, our scheme can be translated to any platform implementing linear optics, such as electronic optics [40], where the degree of indistinguishability can be adjusted by quantum point contacts acting as electronic beam splitters [41]. Additionally, quantum dots appear promising for on-demand generation of single electrons [42], including their initialization and coherent control [43, 44], where tunnel effect in double quantum dots could play the role of the deformation operation generating the indistinguishability [32, 45].

We also envisage possible practical applications of our protocol to measure the EP of anyons in topological quantum computers [4, 46, 47]. Furthermore, the proposed theoretical and experimental setup can be easily adapted to find application in a phase estimation protocol aided by indistinguishability. Indeed, suppose that instead of post-selecting the states where exactly one qubit per region is found with the sLOCC measurement, we discard them by post-selecting the complementary ones. This amounts to project the state $|\psi_D\rangle$ onto the two particle basis $\mathcal{B}_{\mathrm{XX}} = \{|\mathrm{X}\uparrow, \mathrm{X}\uparrow\rangle, |\mathrm{X}\uparrow, \mathrm{X}\downarrow\rangle, |\mathrm{X}\downarrow, \mathrm{X}\downarrow\rangle\}$ with $X = \mathrm{L}, \mathrm{R}$. The resulting state is thus

$$|\psi_{\mathrm{XX}}\rangle = \frac{ll'\,|\mathrm{L}\uparrow, \mathrm{L}\downarrow\rangle + rr'\,|\mathrm{R}\uparrow, \mathrm{R}\downarrow\rangle}{\sqrt{|ll'|^2 + |rr'|^2}}, \qquad (11)$$

which, as can be noticed by rewriting it in the Fock repre-

sentation and disregarding the pseudospin, is equivalent to

$$|\psi_{\rm XX}\rangle = \frac{ll'\,|2,0\rangle + rr'\,|0,2\rangle}{\sqrt{|ll'|^2 + |rr'|^2}}. \tag{12}$$

This is a N00N-like state exploitable for quantum-enhanced phase estimation [48–50]. Adjusting the values of the coefficients one may obtain a N00N state with various weights for the terms $|2,0\rangle$ and $|0,2\rangle$. Remarkably, since the only difference with the EP measurement scheme relies in the postselection, this state can be experimentally generated with the same setup depicted in Fig. 1(b) (excluding the final measurement step).

Finally, we highlight that while the sLOCC operational framework is here exploited to achieve a result of fundamental interest, different practical applications have been designed and experimentally implemented in fields ranging from quantum communication to quantum metrology and sensing, including the generation of entanglement between identical constituents [23, 29], the protection of quantum correlations from detrimental external noise [24, 26–28], and the generation of quantum coherence for metrological applications [25, 31].

This work was supported by the Innovation Program for Quantum Science and Technology (Nos. 2021ZD0301200, 2021ZD0301400), National Natural Science Foundation of China (Nos. 11821404, 61975195, 61725504, U19A2075), Anhui Initiative in Quantum Information Technologies (No. AHY060300), the Fundamental Research Funds for the Central Universities (No. WK2030380017). R.L.F. acknowledges support from European Union – NextGenerationEU – grant MUR D.M. 737/2021 – research project "IRISQ". M.P. and R.L.F. thank Farzam Nosrati for insightful discussions.

Y.W. and M.P. contributed equally to this work

* matteo.piccolini@unipa.it
† ksun678@ustc.edu.cn
‡ jsxu@ustc.edu.cn
§ cfli@ustc.edu.cn
¶ rosario.lofranco@unipa.it

[1] A. Peres, *Quantum Theory: Concepts and Methods* (Springer, 2002).
[2] J. M. Leinaas and J. Myrheim, Il Nuovo Cimento B (1971-1996) **37**, 1-23 (1977).
[3] F. Wilczek, Phys. Rev. Lett. **48**, 1144 (1982).
[4] C. Nayak, S. H. Simon, A. Stern, M. Freedman, and S. DasSarma, Rev. Mod. Phys. **80**, 1083 (2008).
[5] J. Nakamura, S. Liang, G. C. Gardner, and M. J. Manfra, Nat. Phys. **16**, 931 (2020).
[6] H. Bartolomei, M. Kumar, R. Bisognin, A. Marguerite, J. M. Berroir, E. Bocquillon, B. Placais, A. Cavanna, Q. Dong, U. Gennser, *et al.*, Science **368**, 173 (2020).
[7] R. C. Hilborn and C. L. Yuca, Phys. Rev. Lett. **76**, 2844 (1996).
[8] G. Modugno, M. Inguscio, and G. M. Tino, Phys. Rev. Lett. **81**, 4790 (1998).
[9] D. English, V. V. Yashchuk, and D. Budker, Phys. Rev. Lett. **104**, 253604 (2010).
[10] K. Deilamian, J. D. Gillaspy, and D. E. Kelleher, Phys. Rev. Lett. **74**, 4787 (1995).
[11] M. de Angelis, G. Gagliardi, L. Gianfrani, and G. M. Tino, Phys. Rev. Lett. **76**, 2840 (1996).
[12] S. Ospelkaus, K. K. Ni, D. Wang, M. H. G. de Miranda, B. Neyenhuis, G. Quéméner, P. S. Julienne, J. L. Bohn, D. S. Jin, and J. Ye, Science **327**, 853 (2010).
[13] K. Tschernig, C. Müller, M. Smoor, T. Kroh, J. Wolters, O. Benson, K. Busch, and A. Pérez Leija, Nat. Photon. **15**, 671 (2021).
[14] R. Lo Franco, Nat. Photon. **15**, 638 (2021).
[15] M. C. Tichy, F. Mintert, and A. Buchleitner, J. Phys. B: At. Mol. Opt. Phys. **44**, 192001 (2011).
[16] G. C. Ghirardi and L. Marinatto, Phys. Rev. A **70**, 012109 (2004).
[17] A. P. Balachandran, T. R. Govindarajan, A. R. de Queiroz, and A. F. Reyes Lega, Phys. Rev. Lett. **110**, 080503 (2013).
[18] T. Sasaki, T. Ichikawa, and I. Tsutsui, Phys. Rev. A **83**, 012113 (2011).
[19] F. Benatti, R. Floreanini, and U. Marzolino, Ann. Phys. **327**, 1304 (2012).
[20] S. Chin and J. Huh, Phys. Rev. A **99**, 052345 (2019).
[21] R. Lo Franco and G. Compagno, Sci. Rep. **6**, 20603 (2016).
[22] G. Compagno, A. Castellini, and R. Lo Franco, Phil. Trans. R. Soc. A **376**, 20170317 (2018).
[23] R. Lo Franco and G. Compagno, Phys. Rev. Lett. **120**, 240403 (2018).
[24] F. Nosrati, A. Castellini, G. Compagno, and R. Lo Franco, npj Quant. Inf. **6**, 39 (2020).
[25] A. Castellini, R. Lo Franco, L. Lami, A. Winter, G. Adesso, and G. Compagno, Phys. Rev. A **100**, 012308 (2019).
[26] M. Piccolini, F. Nosrati, G. Compagno, P. Livreri, R. Morandotti, and R. Lo Franco, Entropy **23**, 708 (2021).
[27] F. Nosrati, A. Castellini, G. Compagno, and R. Lo Franco, Phys. Rev. A **102**, 062429 (2020).
[28] M. Piccolini, F. Nosrati, R. Morandotti, and R. Lo Franco, Open Systems & Information Dynamics **28**, 2150020 (2021).
[29] K. Sun, Y. Wang, Z. H. Liu, X. Y. Xu, J. S. Xu, C. F. Li, G. C. Guo, A. Castellini, F. Nosrati, G. Compagno, and R. Lo Franco, Opt. Lett. **45**, 6410 (2020).
[30] M. R. Barros, S. Chin, T. Pramanik, H. T. Lim, Y. W. Cho, J. Huh, and Y. S. Kim, Opt. Express **28**, 38083 (2020).
[31] K. Sun, Z. H. Liu, Y. Wang, Z. Y. Hao, X. Y. Xu, J. S. Xu, C. F. Li, G. C. Guo, A. Castellini, L. Lami, A. Winter, G. Adesso, G. Compagno, and R. Lo Franco, PNAS **119**, e2119765119 (2022).
[32] M. Piccolini, F. Nosrati, G. Adesso, R. Morandotti, and R. Lo Franco, Phil. Trans. R. Soc. A, in press. Preprint at arXiv:2205.12136 [quant-ph] (2022).
[33] C. F. Roos, A. Alberti, D. Meschede, P. Hauke, and H. Häffner, Phys. Rev. Lett. **119**, 160401 (2017).
[34] D. F. V. James, P. G. Kwiat, W. J. Munro, and A. G. White, Phys. Rev. A **64**, 052312 (2001).
[35] L. Sansoni, F. Sciarrino, G. Vallone, P. Mataloni,

A. Crespi, R. Ramponi, and R. Osellame, Phys. Rev. Lett. **108**, 010502 (2012).
[36] J. C. Matthews, K. Poulios, J. D. Meinecke, A. Politi, A. Peruzzo, N. Ismail, K. Wörhoff, M. G. Thompson, and J. L. O'Brien, Sci. Rep. **3**, 1539 (2013).
[37] T. Krisnanda, S. Ghosh, T. Paterek, W. Laskowski, and T. C. Liew, Phys. Rev. Applied **18**, 034011 (2022).
[38] S. Taravati and G. V. Eleftheriades, Phys. Rev. Applied **18**, 034082 (2022).
[39] R. Wang, S. He, and H. Luo, Phys. Rev. Applied **18**, 044016 (2022).
[40] C. Bäuerle, D. C. Glattli, T. Meunier, F. Portier, P. Roche, P. Roulleau, S. Takada, and X. Waintal, Rep. Prog. Phys. **81**, 056503 (2018).
[41] E. Bocquillon, V. Freulon, J. M. Berroir, P. Degiovanni, B. Plaçais, A. Cavanna, Y. Jin, and G. Fève, Science **339**, 1054 (2013).
[42] G. Fève, A. Mahé, J. M. Berroir, T. Kontos, B. Placais, D. Glattli, A. Cavanna, B. Etienne, and Y. Jin, Science **316**, 1169 (2007).
[43] D. Press, T. D. Ladd, B. Zhang, and Y. Yamamoto, Nature **456**, 218 (2008).
[44] J. R. Petta, A. C. Johnson, J. M. Taylor, E. A. Laird, A. Yacoby, M. D. Lukin, C. M. Marcus, M. P. Hanson, and A. C. Gossard, Science **309**, 2180 (2005).
[45] R. Hanson, L. P. Kouwenhoven, J. R. Petta, S. Tarucha, and L. M. K. Vandersypen, Rev. Mod. Phys. **79**, 1217 (2007).
[46] A. Y. Kitaev, Ann. Phys. **303**, 2 (2003).
[47] B. Field and T. Simula, Quantum Science and Technology **3**, 045004 (2018).
[48] V. Giovannetti, S. Lloyd, and L. Maccone, Nat. Photon. **5**, 222 (2011).
[49] M. Hiekkamäki, R. F. Barros, M. Ornigotti, and R. Fickler, Nat. Photon. (2022), https://doi.org/10.1038/s41566-022-01077-w.
[50] S. Hong, Y. S. Kim, Y. W. Cho, S. W. Lee, H. Jung, S. Moon, S. W. Han, H. T. Lim, *et al.*, Nat. Commum. **12**, 5211 (2021).